AFGC-ACI-*fib*-RILEM Int. Symposium on Ultra-High Performance Fibre-Reinforced Concrete,
UHPFRC 2017 – October 2-4, 2017, Montpellier, France

EXPERIMENTAL RESEARCH ON THE BEHAVIOUR OF SHORT HEADED STUD IN NON-STEAM-CURED UHPC UNDER TENSILE AND SHEAR LOAD

Qili Sun (1), Jiansheng Fan (1), Xinying Lu (1) and Zhe Wang (1)

(1) Department of Civil Engineering, Key Laboratory of Civil Engineering Safety and Durability of China Education Ministry, Tsinghua University, Beijing, China

Abstract

In recent years, Ultra-High Performance Concrete (UHPC) is more and more widely applied in composite construction and steel structure strengthening due to its super high strength and ductility. However, the mechanical performance of the short headed stud in the interface between UHPC and steel plate hasn't been clearly revealed, which is quite different from that in regular concrete. In this paper, a series of pure-tensile and push-out tests were conducted to investigate the ultimate bearing, crack propagation and failure mode of short headed studs in UHPC. The results showed that the capacity and ductility were both much higher than studs in regular concrete. Besides, current design methods largely underestimate the capacity of UHPC cone failure, thus an assumption of variable angle failure surface mechanism and a modified formula considering the steel fiber quantity were raised based on the experimental results. Finally, a load-slip function was calibrated through the push-out results, which could further be applied in finite element analysis as spring elements.

Résumé

Ces dernières années, le béton fibré à ultra-hautes performances (BFUP) a été de plus en plus employé en construction mixte et en renforcement de structures en acier en raison de sa résistance et de sa ductilité. Cependant, les performances mécaniques des mini-goujons à l'interface entre le BFUP et la semelle d'acier n'ont pas été clairement documentées, contrairement au cas du béton ordinaire. Dans cet article, une série de tests de résistance en traction pure et en cisaillement a été réalisée pour évaluer la capacité ultime, la propagation des fissures et le mode de rupture des mini-goujons dans le BFUP. Les résultats montrent que la capacité et la ductilité dépassent nettement celle des goujons dans le béton ordinaire. De plus, les méthodes de calcul actuelles sous-estiment largement la charge de rupture par cône dans le BFUP ; l'hypothèse d'un mécanisme de rupture avec une surface d'angle variable et une formule modifiée tenant compte de la quantité de fibres d'acier ont donc été proposées sur la base de ces résultats expérimentaux. Enfin, une fonction charge-glissement a été calibrée grâce aux résultats des essais de cisaillement, qui pourrait à l'avenir être appliquée à des éléments ressorts dans une analyse aux éléments finis.

1. INTRODUCTION

Ultra-high performance concrete (UHPC) is a type of cement-based composite material with super high strength, toughness and durability. Its components could minimize inner defects because of their high fineness and activity. Currently, plenty of sufficient studies on the production, properties, and engineering application of UHPC have been reported [1, 2].

By combining UHPC with steel structure, a superior new composite structure form occurred, which could be applied in large-span bridge construction. Generally, a UHPC composite bridge deck could feasibly have a thinner concrete cross-section than a conventional one based on strength design [3]. Consequently, the headed studs in the interface needed to be very short, whose mechanical behaviour in UHPC under complicated loading state would significantly influence the structure performance. Kim et al. [3] conducted 15 push-out tests of stud shear connectors embedded in UHPC slab, and concluded that the overall height-to-diameter ratio of stud could be reduced to 3.1 without loss of shear capacity.

To the benefit of construction convenience and the application of non-steamed-cured UHPC, in this paper, a special UHPC mix proportion with properties of early-strength and low shrinkage was adopted. A series of pure-tensile and push-out tests were carried out to investigate the ultimate bearing, crack propagation and failure mode of headed studs in UHPC. Furthermore, modified tensile capacity formula and load-slip function in UHPC were proposed and calibrated with the test results. The results of this paper provide an effective reference for UHPC-steel composite bridge deck design.

2. EXPERIMENTAL PROGRAM

The diameter of investigated shear stud was 13 mm, with a length of 35 mm or 60 mm for parametric study as is shown in Fig. 1. The ultimate strength of the stud bar steel was 528.3 MPa obtained from following pure-tensile test.

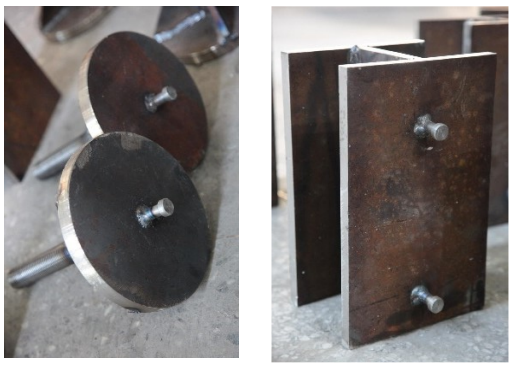

Figure 1: Steel structure parts of specimens (a) pure-tensile specimen (b) push-out specimen

2.1 Pure-tensile test

In order to ensure the stress well-distributed in the interface, a 200-mm-diameter cylinder specimen was designed for the pure-tensile test as is presented in Fig. 1a and Fig. 2. The interface to be investigated was located in the lower position, whose steel plate part was welded with bottom clamping structure. While the top of the specimen was connected with upper clamping structure through pre-embedded bolts. Specially, to eliminate external affect, 40-mm-thick pure UHPC was reserved between the stud head and the end of embedded bolts.

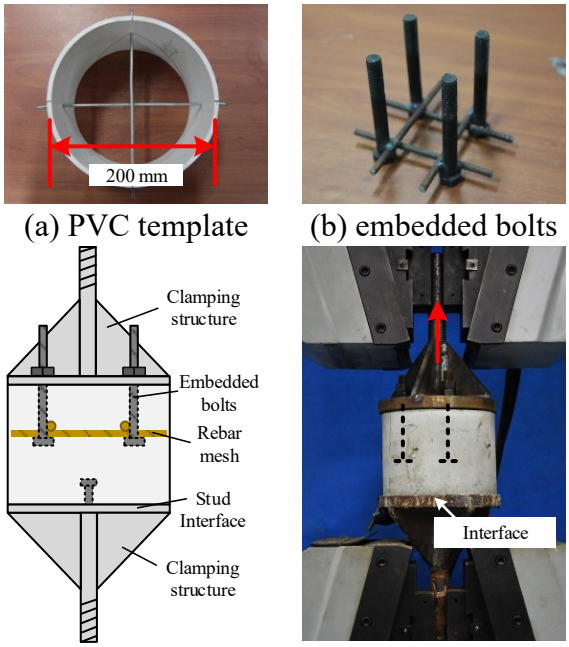

(a) PVC template (b) embedded bolts

(c) before casting (d) testing setup

Figure 2: Specimen preparation and loading method.

Table 1. Variable of the pure-tensile specimens.

Group	Name	v_f (%)	h (mm)	Adhesion	Amount
1	PTHS0	0	35	Nature	2
2	PTHS1	1	35	Nature	3
3	PTHS	2	35	Nature	5
4	PTHSP	2	35	Separated by plastic sheet	2
5	PTHSL	2	60	Nature	3

A PVC pipe segment was adopted as the UHPC casting template, which was perforated and threaded by two cross iron wires to control the embedded depth of the bolts which had already been welded together using steel rebar (Fig. 2). All of the specimens were tested using a 1000-kN tensile tester. Note that the specimen was gripped by the tester before the bolts were screwed, so that the forces in the embedded bolts would be well-distributed to avoid bending moment. A displacement meter was installed at the investigated interface to record the uplift value. Parametric analysis was carried out considering the length of stud h, the volume ratio of steel fiber v_f and the adhesion condition in the interface. In total, 15 specimens of pure-tensile tests were conducted as is listed in Table 1 (PT- presented for pure-tensile, HS for headed stud and the last symbol referred to the variable). Another 2 PTHS specimens were tested because of the unusual adhesion of the first batch, which will be discussed later.

2.2 Push-out tests

Considering the particularity of UHPC and the design recommendations in Eurocode 4 Part 1-1 [5], the detailed geometry of the push-out specimen is depicted in Fig. 4. Different from regular one, the specimen in this paper was divided into two halves to ensure uniform age and casting quality of two UHPC slabs. After one-week standard curing in the lab, the two parts

were connected together through batten plates and bolts. Meanwhile, two displacement meters were set to monitor the slip in both interfaces, whose readings were similar during the test which validated the integration of the specimen. The result at the first failed side was used in subsequent analysis.

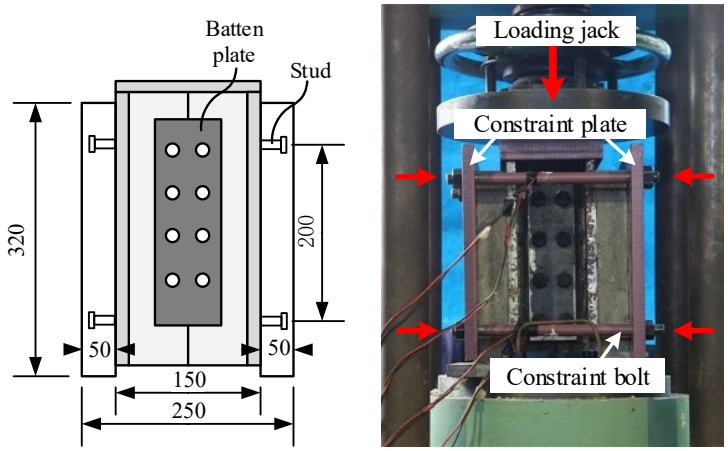

Figure 3: Push-out specimen and the test method. (a) push-out specimen (b) testing pattern

In order to research the effect of lateral constraint, two 20 mm thick steel plates and four prestressed bolts with a diameter of 20 mm were designed to limit the separation of the UHPC and the steel structure during the tests (Fig. 3). In the push-out test, two shear studs were welded onto both sides as is presented in Fig. 3. The specimens were divided into two groups (POHS and POHSC, where PO- represented push-out and -C referred to constraint), each containing three specimens. All of the push-out specimens were tested using a 2000-kN compression tester.

2.3 Material properties

Table 2. Mix proportion of non-steam-cured UHPC.

component	unit	Amount
Sulphate aluminium cement	kg/m^3	1022
Mineral admixture	kg/m^3	147
Quartz sand	kg/m^3	886
Suspending agent	kg/m^3	73.8
Superplasticizer	kg/m^3	5.7
Additive (shrinkage reducer, defoamer etc.)	kg/m^3	13
Water	kg/m^3	215
Steel fiber （2%）	kg/m^3	156

The UHPC investigated in this paper was mixed specially, consisting of sulphate aluminium cement and shrinkage reducer, which was often applied in emergency repair due to its early high strength. Meanwhile, its low shrinkage property avoided later crack, which was suitable for non-steam curing method. A type of fiber with a length of 13 mm and a diameter of 0.2 mm was added, whose volume ratio ranged from 0 to 2% in this paper.

Table 2 showed the mix proportion, with a ratio of water to cementitious material equalling 0.18.

The material properties of steel plate, stud and non-steam-cured UHPC are summarized in Table 3. The UHPC specimen for compression test was 100 mm cubic and the strength became stable after 7 days which validated its early strength property. The flexural strength f_r was obtained through three-point bending test with the specimen geometry of 100×100×400 mm, while the tensile strength f_t through 20×100×200 mm direct tensile test. The elastic modulus of the UHPC material was about 40.3 GPa, hardly changing with the fiber quantity.

Table 3. Material properties.

Material	Applications	Thickness (mm)	f_y (MPa)	f_u (MPa)
Steel	Stud	ϕ13	/	528.3
UHPC	Steel fiber (%)	f_{cu} (MPa)	f_r (MPa)	f_t (MPa)
	0	103.8	8.3	2.3
	1	108.3	10.3	2.5
	2	119.3	14.5	4.7

3. TEST OBSERVATIONS AND RESULTS

3.1 Pure-tensile tests

Generally, when a stud anchor sustained tensile load in concrete, either concrete breaking or stud rupturing might appear, depending on the capacity relationship of the stud and concrete. In short stud condition, the concrete was more likely to break. In fact, except for two weld foot failure specimens, all of the 35-mm-stud ones showed concrete destruction, wherein three failure modes were observed as are presented in Fig. 4.

The concrete cone failure was the most common phenomenon, where after the adhesion between the UHPC and steel plate failed, the initial inner crack occurred near the head of stud, and hence propagated along certain angle towards the interface as the uplift increased. After reaching the peak point, the bearing load decreased gradually, forming a concrete cone around the stud (Fig, 4a). The failure behaviour became more ductile with the increase of steel fiber, presenting an evident positive relationship with the ultimate capacity value. Specially, when no fiber was added (PTHS0), the specimen failed once uplift arose showing brittle failure, and the conical crack surface was more flat and smooth as is demonstrated in Fig. 5a.

(a) concrete cone failure (b) splitting failure (c) combine failure

Figure 4: Three concrete failure modes in the pure-tensile tests.

(a) no-fiber cone failure (b) strong adhesion (c) weld foot failure

Figure 5: Special conditions observed in the tests.

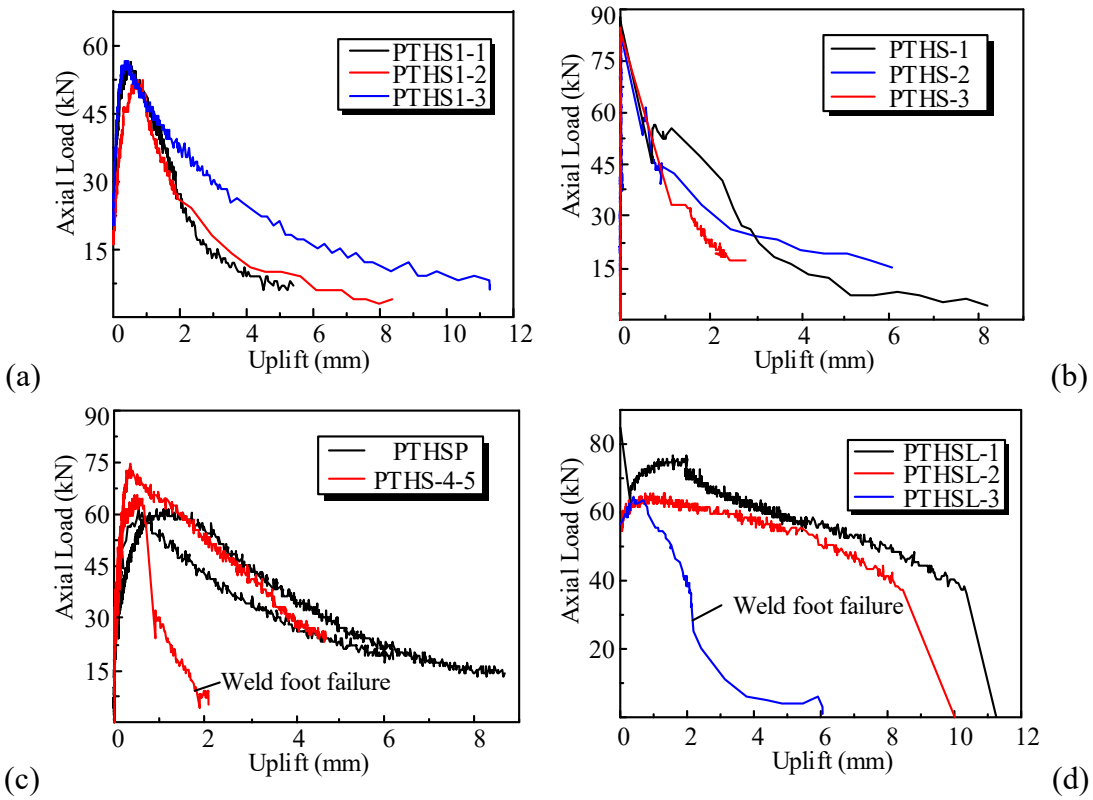

Figure 6: Axial load-uplift curves of the pure-tensile tests.

Similarly, splitting failure also had evident ductility, where UHPC broken into several pieces, and the stud slid out alone from the crack gap. However, compared with UHPC splitting failure, the combined mode was more common as is shown in Fig 4c. However, the three failure types shared similar mechanical behaviour and ultimate capacity, it could be implied that the cone crack might be the initial stage and the sustained tensile stress of UHPC in the axial symmetry plane was close to circular stress. Note that the concrete cone tended to became smaller or turn into splitting or combined when the steel fiber quantity increased.

In addition, the interface adhesion had an evident impact on the tensile behaviour of stud anchor, which was mainly influenced by the interface roughness and concrete curing age. For instance, the first batch of PTHS group showed a different performance: the crack did not appear until suddenly the adhesion failed, then the headed stud began to play a role and the bearing load decreasing slowly. When using plastic to isolate the interface, the ultimate capacity was a little lower as is presented in Fig. 6c.

In the long headed studs group (PTHSL), the curve presented a yield stage until the stud bar necked and ruptured. Fig. 6 and Table 4 presented the results of pure-tensile tests, where the weld foot failure results weren't taken into account.

Table 4. Pure-tensile test results.

	Fiber volume ratio (%)	Stud height (mm)	Average ultimate load (kN)
PTHS0	0	h =35	25.7
PTHS1	1	h =35	55.5
PTHS-1-3	2	h =35	85.1
PTHS-4-5	2	h =35	74.7
PTHSP	2	h =35	62.0
PTHSL	2	h =60	70.1*

Note: *Results when the stud bar reached ultimate bearing capacity.

3.2 Push-out tests

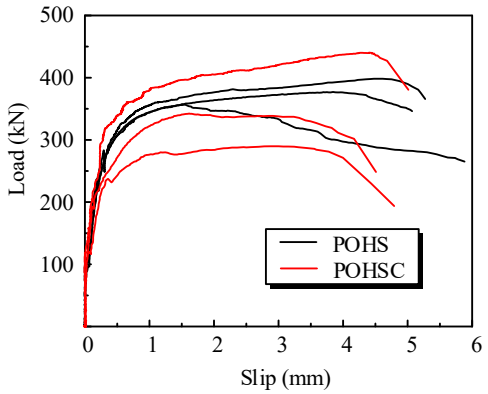

Figure 7: Load-slip curve of push-out tests.

Table 5. Push-out test results.

	S_u (mm)	S_{peak} (mm)	P_u (kN)	P_{2mm} (kN)	P_{2mm}/P_u
POHS-1	5.1	3.8	94.3	91.0	96.5%
POHS-2	5.3	4.5	99.6	94.1	94.5%
POHS-3	5.9	1.5	89.2	86.7	97.2%
POHSC-1	4.8	2.9	72.5	71.0	98.0%
POHSC-2	4.5	1.6	85.6	84.7	98.9%
POHSC-3	5.0	4.4	110.1	101.3	92.0%

The push-out tests results of the headed stud specimens were shown in Fig. 7 and Table 5, and the test process presented relatively ductile behaviour. As the load increased, the headed stud ruptured at the foot caused by shear force. It was discovered after tests that the UHPC around the studs was crushed (Fig. 7a), but the entire UHPC slab was still in good condition, without any visible cracks, which indicated that regular short studs did not have sufficient strength to take full advantage of UHPC's ultra-high property, and those with larger capacity might be more suitable.

The average load capacity of specimens with lateral constraint was 89.36 kN per stud, 5.3% lower than that without constraint, but much larger than the design value in Eurocode-4 [5]. It could be explained that when no lateral constraint existed, a compressive concrete wedge would form before the weld foot because of the ultra-high strength of UHPC as the load arises (Fig 8) [6]. Hence the concrete slab together with the load moved upwards, resulting in that the stud bar sustained both tensile force P_T and shear force until finally ruptured. The total capacity was the sum of the resistant force of stud T and the friction on the wedge P_f. However, when constraint was applied, the slab couldn't move freely, thus the weld foot bore all the shear force, note that all the studs were weld all around on the steel plate rather than using arc welding method. Thus the peak load equalled to the capacity of the weld foot, which might be lower than the total of stud shear capacity and friction on the concrete wedge. Besides, the average lateral force was 54kN among the three POHSC specimens.

(a) without constraint (b) with constraint (c) load carrying mechanism

Figure 8: Push-out failure photos and stud load carrying model.

Nevertheless, the characteristic slip values of the studs were all smaller than 6mm as was required in Eurocode-4 [5], which implied that this provision might be not suitable for short stud in UHPC-steel composite structure.

4. DISCUSSION

4.1 Tensile capacity of headed stud connection

The classical calculation method of stud anchor in concrete was CCD raised by Fuchs [7], based on plenty of test data, which was also the theoretic model of AIC318 [8].

However, when applied to calculate the anchor capacity of headed stud in UHPC with fiber, evident underestimation occurred, so were other theories and codes (Table 6), which would cause huge waste in practice. Thus, a modified model should be raised relevant to the fiber quantity, wherein the authors believed that the concrete tensile strength should be applied instead of compression strength. Based on the test observation depicted in Fig. 9, a variable angle failure surface model was raised, which implied that the radius of the projection plane of the concrete cone was larger than twice of the efficient embedded depth h_{ef}. Thus a parameter k was proposed to describe the relationship between fiber quantity v_f (%) (within 2%) and the influential region of stud. Finally, a modified formula based on Farrow and Klingner's study [9] was as follows:

$$T = kf_t\pi\ h_{ef}^2 \quad (1)$$

$$k = -2.8v_f+12.5$$

Table 6 Comparison of classical theory, codes and new method with test results

(kN)	Test result	Fuchs[7]	ACI 318[8]	Farrow[9]	Equation (1)
PTHS0	25.7	26.6	19.9	23.9	25.8
PTHS1	55.5	27.2	20.3	24.4	55.5
PTHS	74.7	28.5	21.3	25.6	74.3

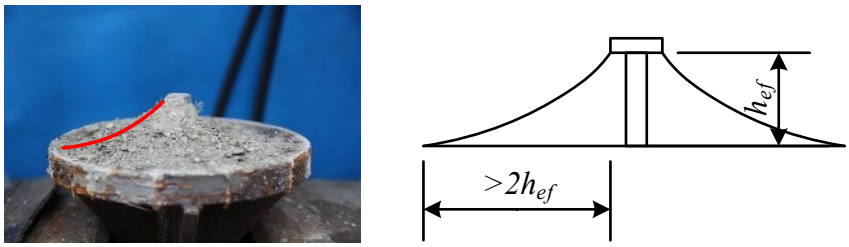

Figure 9: Variable angle failure surface of UHPC cone failure.

4.2 Headed stud load-slip function

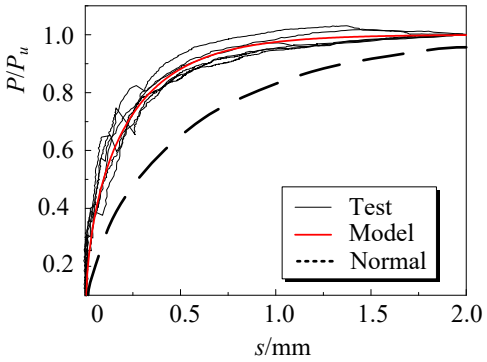

Figure 10: Comparison of the mathematical model and the test results.

To address an applicable between the shear load (V) and relative slip(s) relationship of the stud in UHPC, the bearing load were normalized by corresponding capacity when the slip was 2mm. As is demonstrated in Table 6, the bearing capacity at 2mm slip was close to ultimate value. Two key parameters in the classical slip-load function of headed stud raised by Ollgaard [6] were calibrated by six push-out tests.

$$V = V_u(1\text{-}e^{-ns})^m \quad (2)$$

where V_u is the shear capacity of the stud and n=3mm^{-1} & m=0.5 for the headed stud case in UHPC, considering application convenience and conservative estimation. The exponential function based mathematical model of the load-slip relationship was in accordance with the test curves (Fig. 10). And the curves indicated that the initial stiffness was much larger in UHPC than in regular concrete (n=1mm^{-1}， m=0.558 [11]), which could be explained that because of the ultra-high properties of UHPC, the concrete near the stud was not so easy to be crushed. Kim et al. [3] and Hegger [6] have observed similar phenomena.

5. CONCLUSION AND RECOMMENDATION

In this paper, a series of pure-tensile and push-out tests to investigate the mechanical behaviour of headed stud in non-steam-cured UHPC were conducted. The main conclusions of this study are summarized as follows:

- Short headed stud showed relative ductility in both pure-tensile and push-out tests, although which couldn't meet the slip requirement of Eurocode-4 design code. Therefore, other measure should be used to resolve this ductility issue in order to use stud shear connectors for a thin UHPC slab. Besides, current codes and classical theories underestimated the capacity of headed stud in UHPC under both loading conditions.
- A modified anchor capacity calculation formula for headed stud in UHPC were raised based on test results, taking the influence of fiber quantity into consideration.
- Furthermore, a load-slip relationship function for headed stud in UHPC was calibrated, which could further be applied in finite element analysis as spring elements or to define the parameters of interface contact.

ACKNOWLEDGEMENT

This work was financially supported by the National Natural Science Foundation of China (51478245).

REFERENCES

[1] Graybeal, B. A., 'Material property characterization of ultra-high performance concrete', US Department of Transportation, Federal Highway Administration, Publication No. FHWA-HRT-06-103. 2006.

[2] Walraven, J., 'High performance concrete: a material with a large potential', *Journal of Advanced Concrete Technology*, **7**(2) (2009) 145-156.

[3] Kim, J. S., Kwark, J., Joh, C., et al., 'Headed stud shear connector for thin ultrahigh-performance concrete bridge deck', *Journal of Constructional Steel Research* **108** (2015),23–30.

[4] Shao, X. D., Yi, D. T., Huang, Z. Y., et al., 'Basic Performance of the Composite Deck System Composed of Orthotropic Steel Deck and Ultrathin RPC Layer', *Journal of Bridge Engineering* **18** (5) (2013) 417-428.

[5] EN 1994-1-1:2004, 'Eurocode 4: Design of composite and concrete structures Part 1-1: General rules and rules for buildings', European Committee for Standardization, 2004.

[6] Hegger, J., 'Push-out Tests on Headed Studs in High-Strength Concrete', International Symposium on the Utilization of High Strength/high-Performance Concrete. 2005.

[7] Fuchs, W., Eligehausen, R., Breen, J. E., 'Concrete capacity design (CCD) approach for fastening to concrete', *ACI Structural Journal* **92**(1) (1995) 73-94.

[8] 'Building Code Requirements for Structural Concrete (ACI 318-11) and Commentary', American Concrete Institute. 2011.

[9] Farrow, C. B., Klingner, R. E., 'Tensile capacity of anchors with partial or overlapping failure surfaces: Evaluation of existing formulas on an LRFD basis', *ACI Structural Journal* **92**(6) (1995) 698-710.

[10] Ollgaard, J., Slutter, R., Fisher, J., 'Shear strength of stud connectors in lightweight and normal-weight concrete', *AISC Engineering Journal* **8** (2) (1971) 55-64, 1971.

[11] Tao, M. X., Nie, J. G., 'Nonlinear finite element analysis of prestressed continuous steel-concrete composite beams', *China Civil Engineering Journal* **44** (2) (2011) 8-20. (in Chinese)